

Electronic Supplementary Information

Room Temperature Solution Processed Tungsten Carbide As An Efficient Hole Extraction Layer for Organic Photovoltaics

Wei Cui,^{†a} Zhongwei Wu,^{†a} Changhai Liu,^a Mingxing Wu,^b Tingli Ma,^b Suidong Wang,^a Shuit-Tong Lee,^a Baoquan Sun^{*,a}

^aJiangsu Key Laboratory for Carbon-Based Functional Materials & Devices, Institute of Functional Nano & Soft Materials (FUNSOM), Soochow University, Suzhou 215123, P. R. China

^bState Key Laboratory of Fine Chemicals, Dalian University of Technology, No. 2 Linggong Road, Ganjingzi District, Dalian City, Liaoning Province, P. R. China 116024

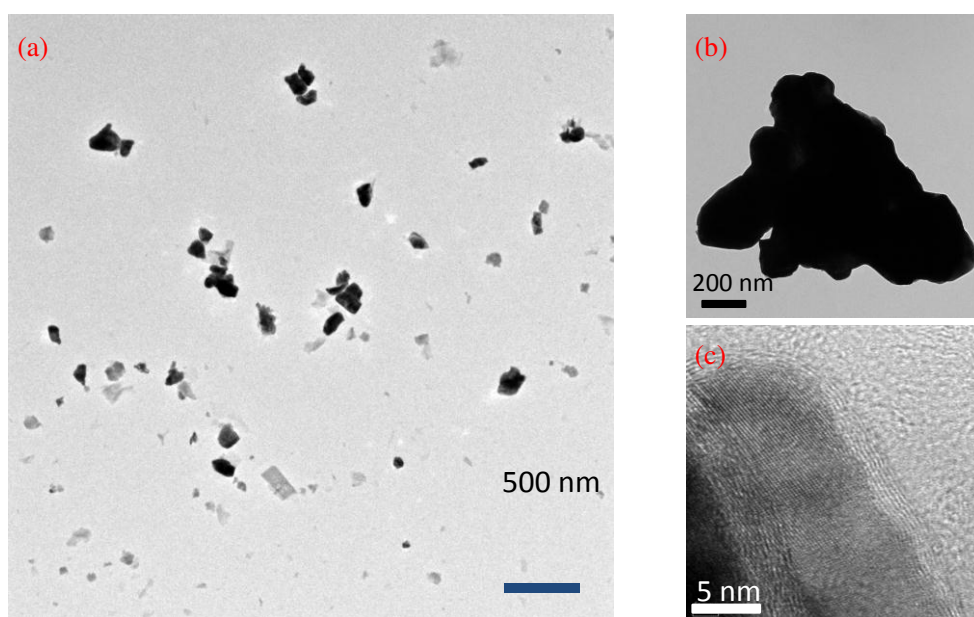


Figure S1 TEM images of (a) the WC nanoparticles after ultrasonication, (b) WC bulk and (c) nanoparticle.

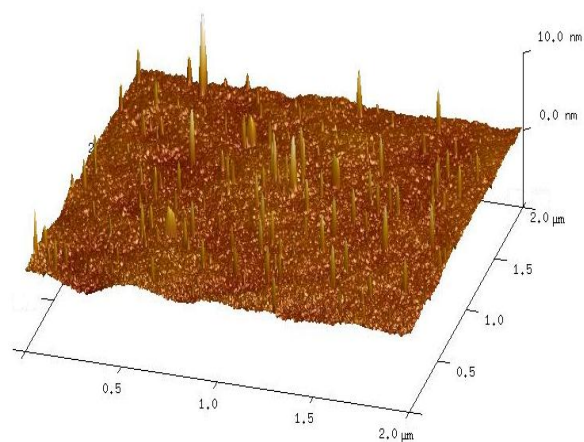


Figure S2 AFM topographic 3-dimension image of WC nanoparticles on a planar silicon substrate. The size of these images was 2 μm x 2 μm.

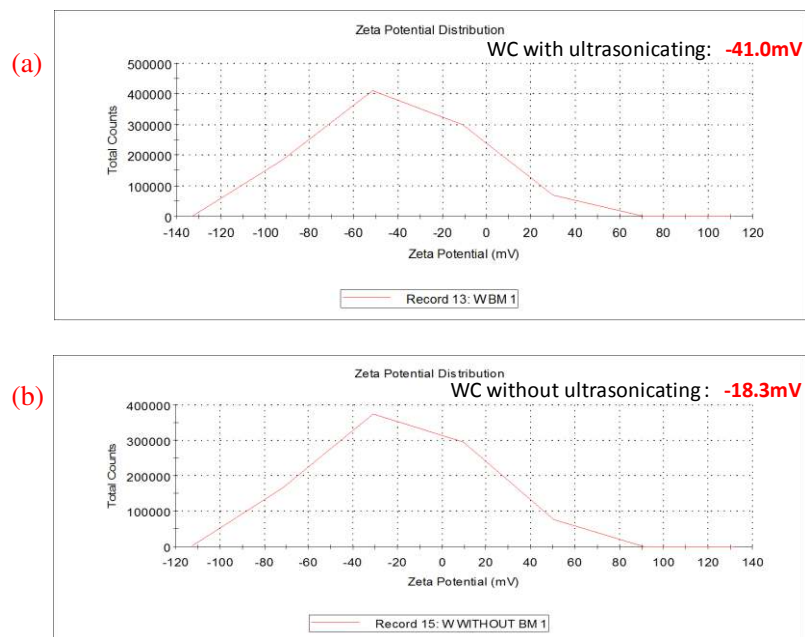


Figure S3 Zeta potential values of WC nanoparticle (a) with and (b) without ultrasonication treatment in isopropanol.

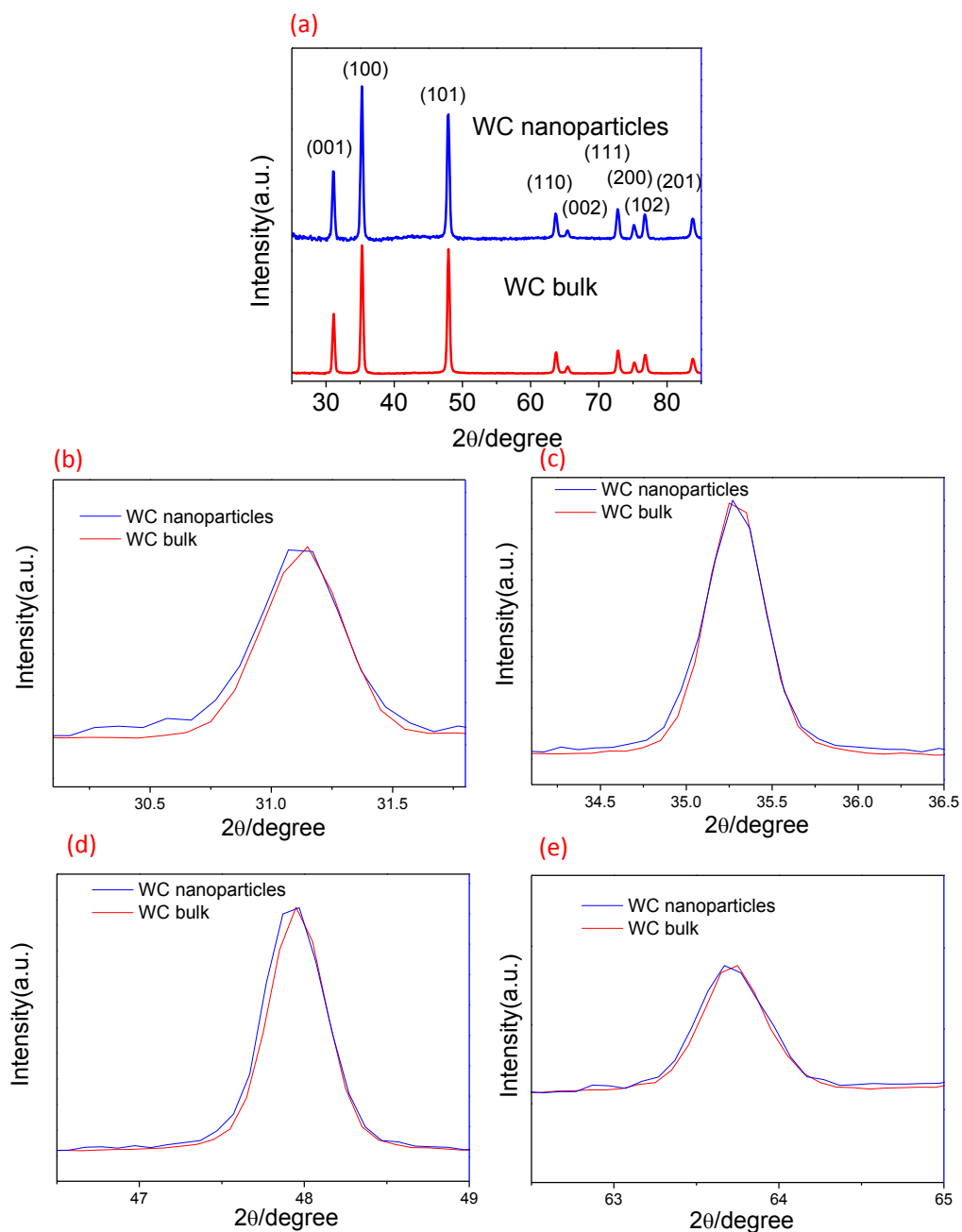


Figure S4 (a) XRD patterns of WC bulks and nanoparticles. (b), (c), (d) and (e) represented the zoom-in XRD patterns of (001) (100) (101) (110) faces in (a), respectively.

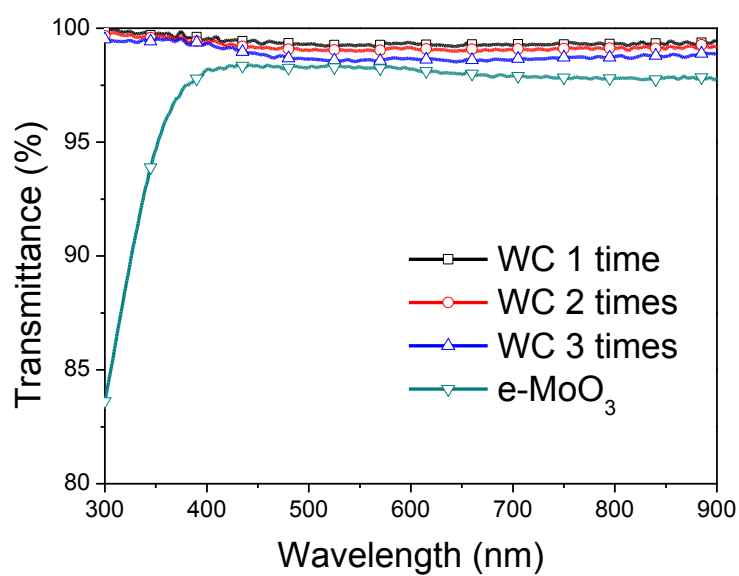


Figure S5 Transmittance spectra of e-MoO₃ film and WC ones prepared by multiple spin-coating times.

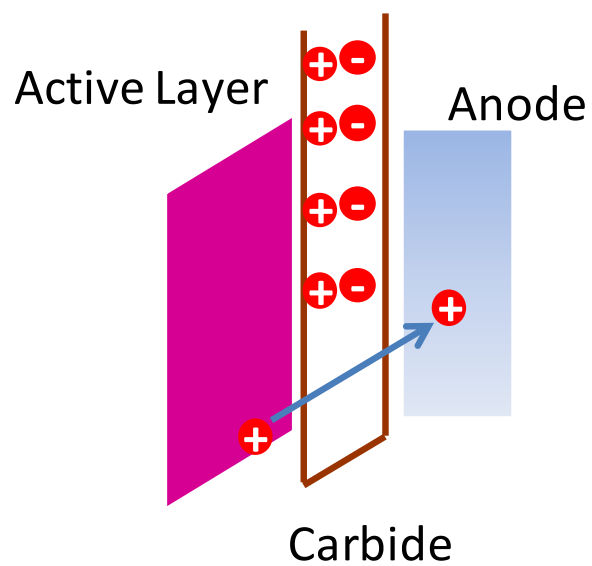


Figure S6 The cartoon model of energy band structure, the WC interlayer under short-circuit conditions at zero external applied bias based on the probed surface dipole.

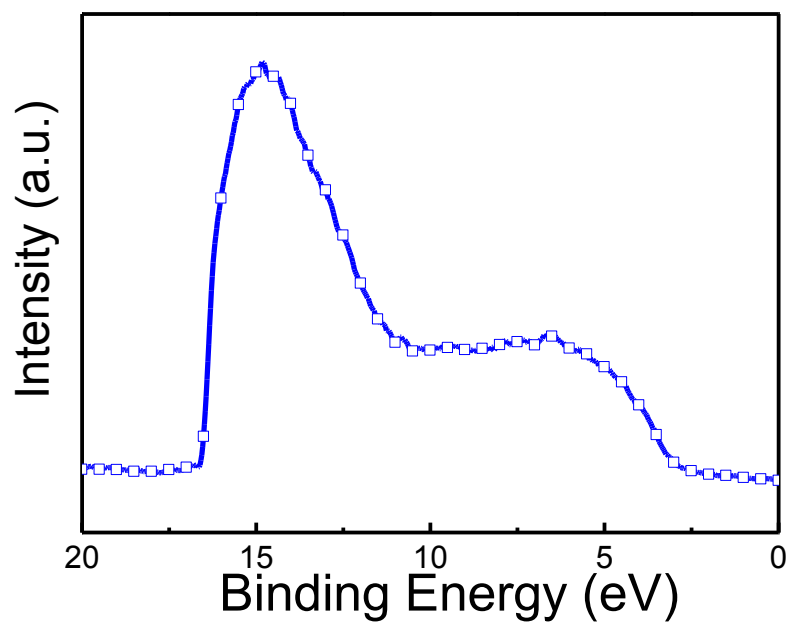


Figure S7 UPS spectra of WC on indium substrate.

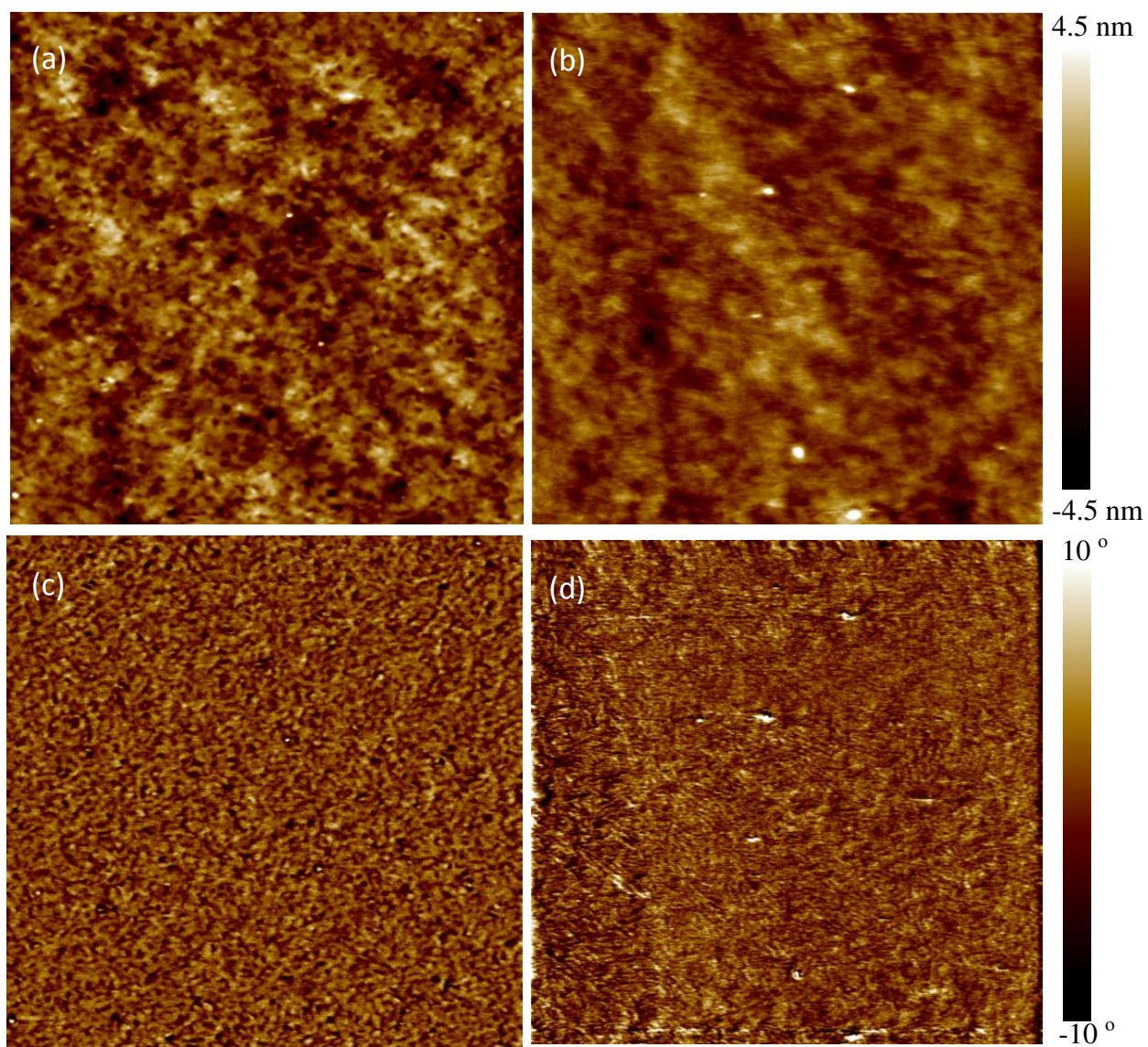


Figure S8 AFM images of P3HT:PC₆₁BM films with WC film deposited one time (a) Height and (c) Phase; (b) Height and (d) Phase with WC film deposited by repeated two times.

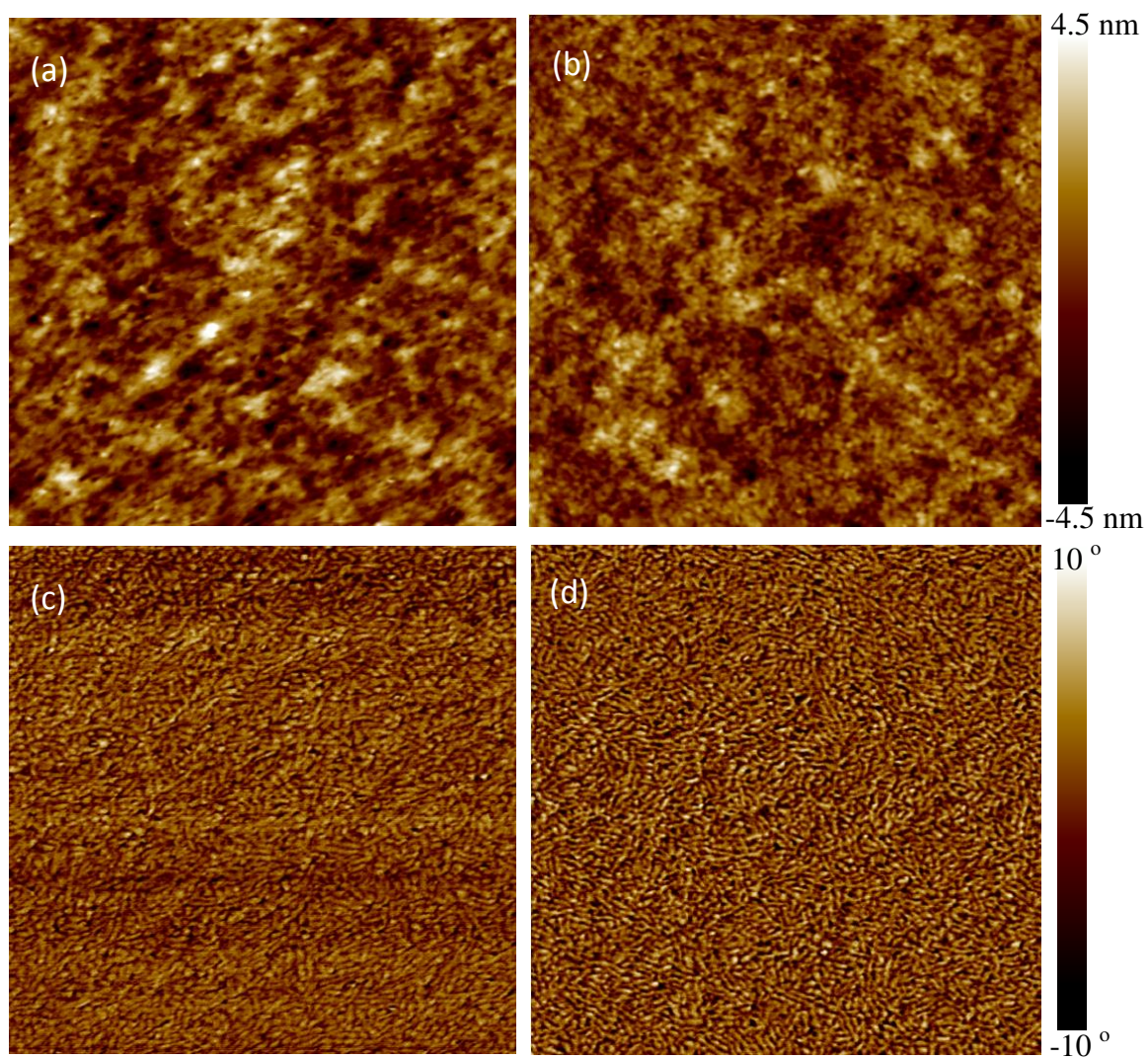


Figure S9 AFM images of P3HT:PC₆₁BM films with spin-coating isopropanol once (a) Height and (c) Phase; (b) Height and (d) Phase with spin-coating isopropanol in three times.

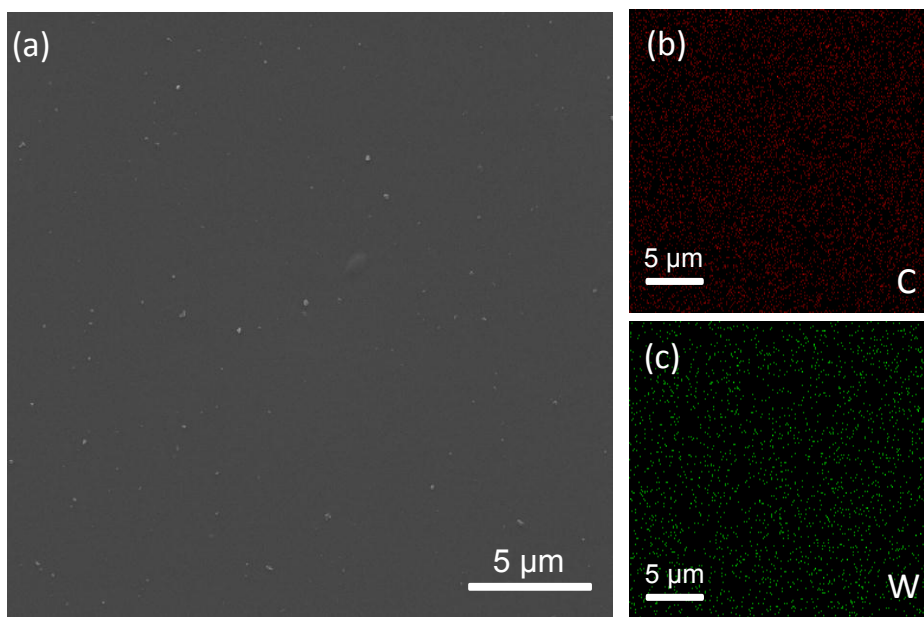


Figure S10 (a) SEM image of the WC film deposited on P3HT:PCBM layer by spin-coating for 3 times, and corresponding elemental mapping images of (b) carbon and (c) tungsten by energy-dispersive X-ray (EDX) spectroscopy, indicating the active layer were fully covered with the WC nanoparticles.

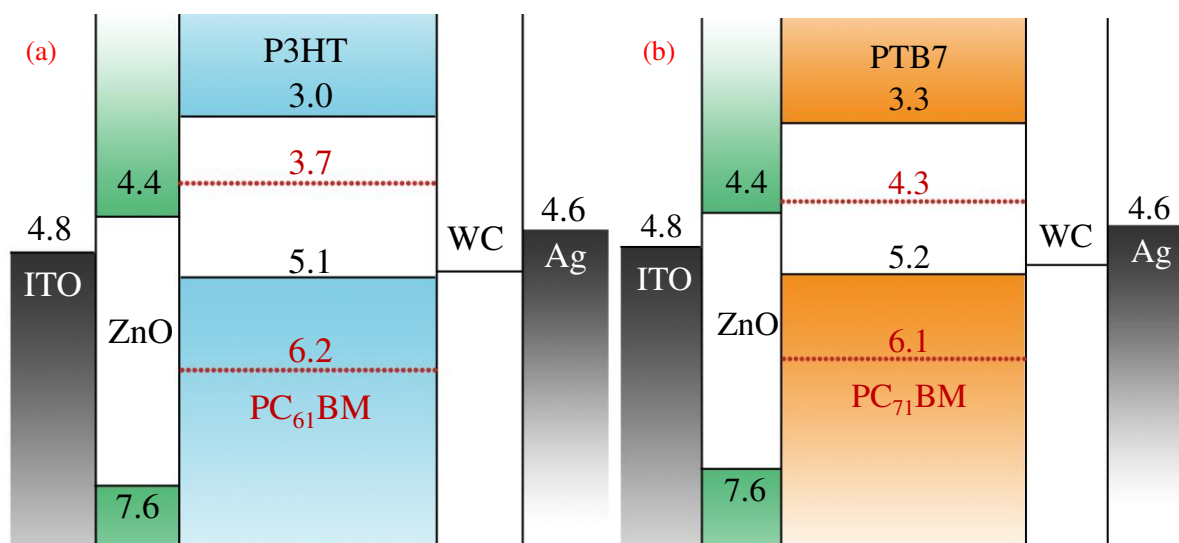


Figure S11 The band structures of the devices with WC anode buffer layers. (a) ITO/ZnO/P3HT:PC₆₁BM/WC/Ag, (b) ITO/ZnO/PTB7:PC₇₁BM/WC/Ag.

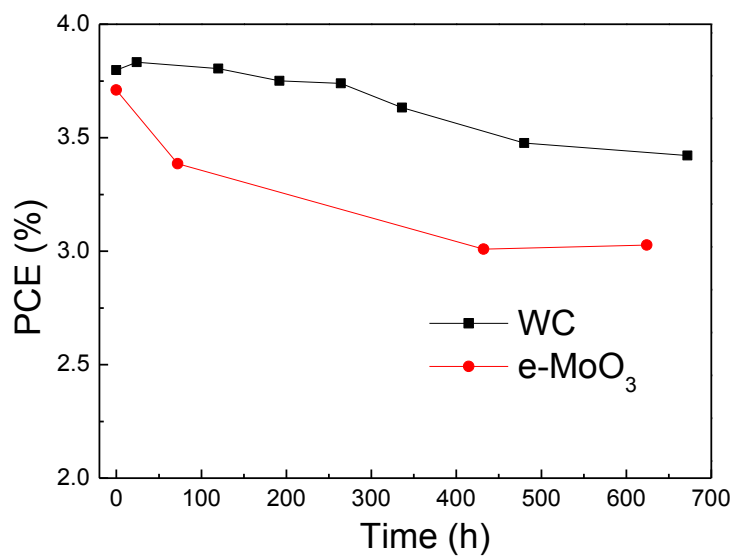


Figure S12 PCEs as a function of storage time for P3HT:PC₆₁BM solar cells based on different hole extraction layer of solution-processed WC and vacuum deposited MoO₃ in air under ambient conditions (no encapsulation).

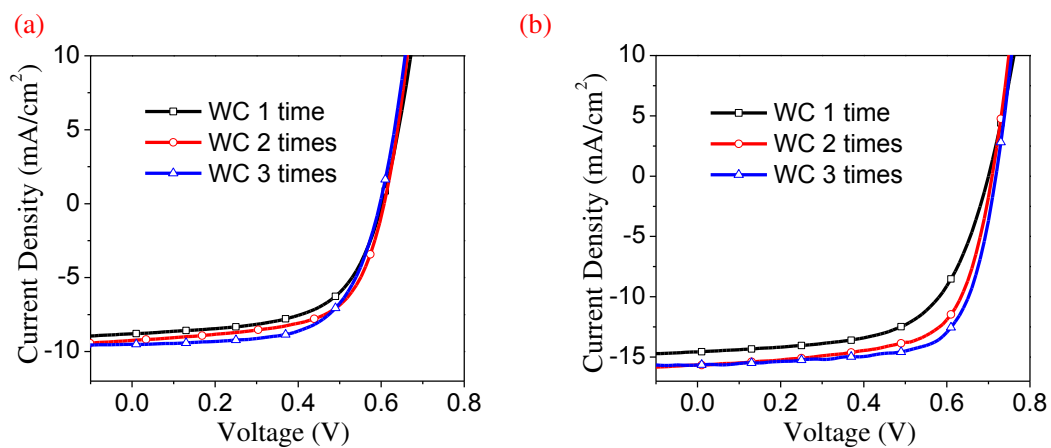


Figure S13 J-V data for inverted solar cell based on (a) P3HT:PC₆₁BM and (b) PTB7: PC₇₁BM with WC buffer layers fabricated by different spin-coating times.

	Spin-coating times	V _{oc} (V)	J _{sc} (mA cm ⁻²)	FF	PCE (%)
P3HT:PC ₆₀ BM	1	0.60	8.78	0.60	3.16
	2	0.60	9.25	0.63	3.50
	3	0.60	9.51	0.64	3.65
PTB7:PC ₇₁ BM	1	0.70	14.55	0.61	6.21
	2	0.70	15.66	0.67	7.3
	3	0.71	15.64	0.71	7.87

Table S1 Summary of electric output characteristics of the inverted solar cells with WC buffer layers fabricated by different spin-coating times.

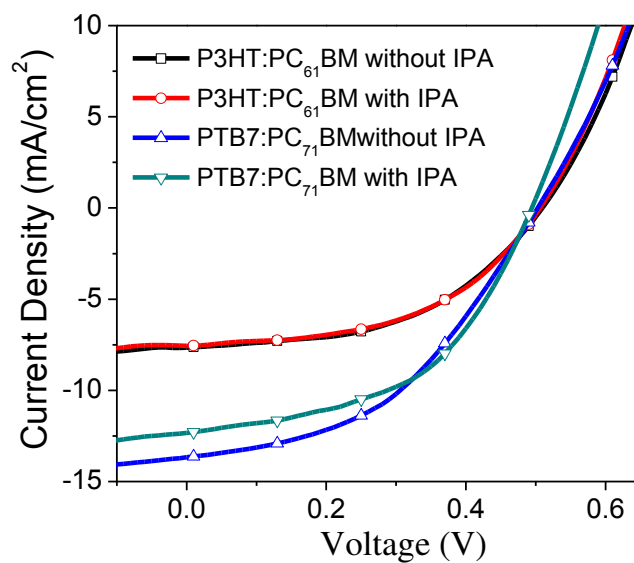


Figure S14 J-V curves of the devices based on P3HT:PC₆₁BM (PTB7: PC₇₁BM) with and without isopropanol treatment. Neither MoO₃ nor WC is inserted between active layer and silver electrodes. The device structures were either ITO/ZnO/P3HT:PC₆₁BM/Ag or ITO/ZnO/PTB7:PC₇₁BM/Ag.

	V_{oc} (V)	J_{sc} (mA cm^{-2})	FF	PCE (%)
P3HT:PC ₆₁ BM without IPA	0.50	7.64	0.50	1.91
P3HT:PC ₆₁ BM with IPA	0.50	7.54	0.51	1.90
PTB7:PC ₇₁ BM without IPA	0.50	13.64	0.45	3.06
PTB7:PC ₇₁ BM with IPA	0.50	12.29	0.51	3.05

Table S2 Electric output characteristics of the devices based on P3HT:PC₆₁BM (PTB7: PC₇₁BM) with and without isopropanol treatment. Neither MoO₃ nor WC was inserted between active layer and silver electrodes. The device structures were either ITO/ZnO/P3HT:PC₆₁BM/Ag or ITO/ZnO/PTB7:PC₇₁BM/Ag.